# The VIIRS M9 Channel And The Development of VIIRS Cirrus Reflectance Algorithm

Bo-Cai Gao and Rong-Rong Li

June 2016

Remote Sensing Division, Code 7230
Naval Research Laboratory, Washington, DC USA

# INTRODUCTION

- Brief descriptions on MODIS and VIIRS cirrus detecting channels
- The cirrus reflectance algorithm
- Sample observations from VIIRS M9 channel images
- Upgrades to the VIIRS cirrus reflectance algorithm
- Summary

# Historical Development With MODIS 1.38-μm Cirrus Detecting Channel

Sample AVIRIS Images

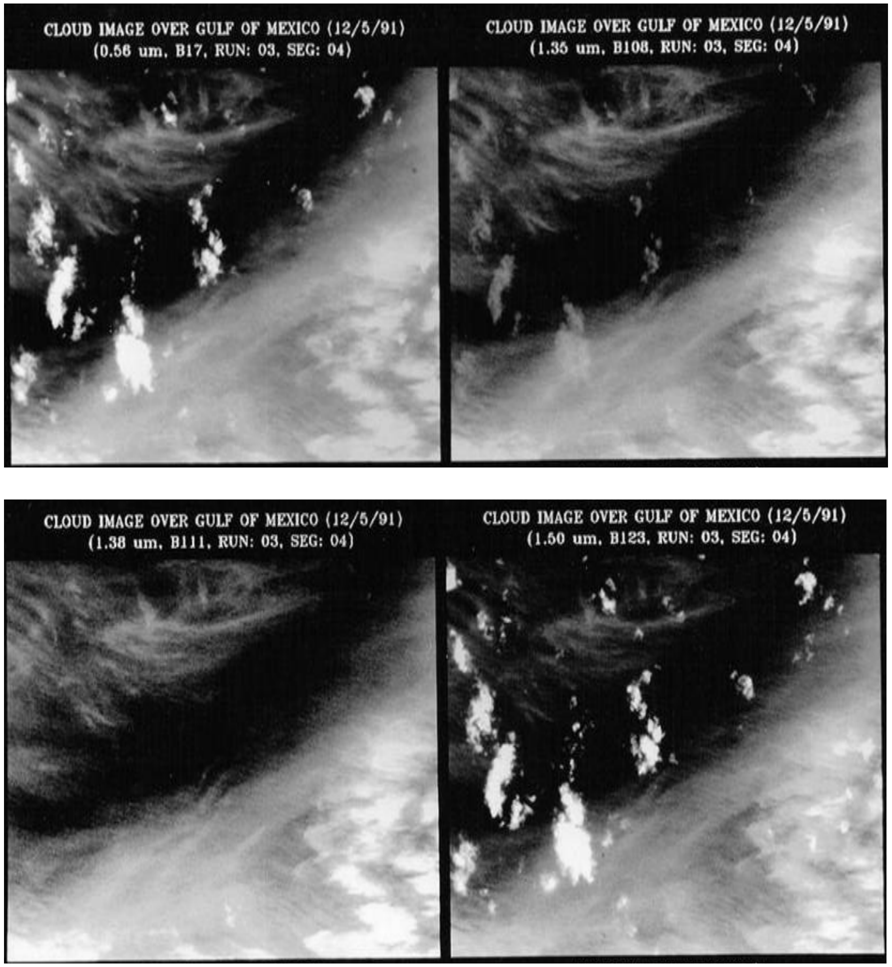


Sample AVIRIS Cirrus Spectra
& MODIS Channels

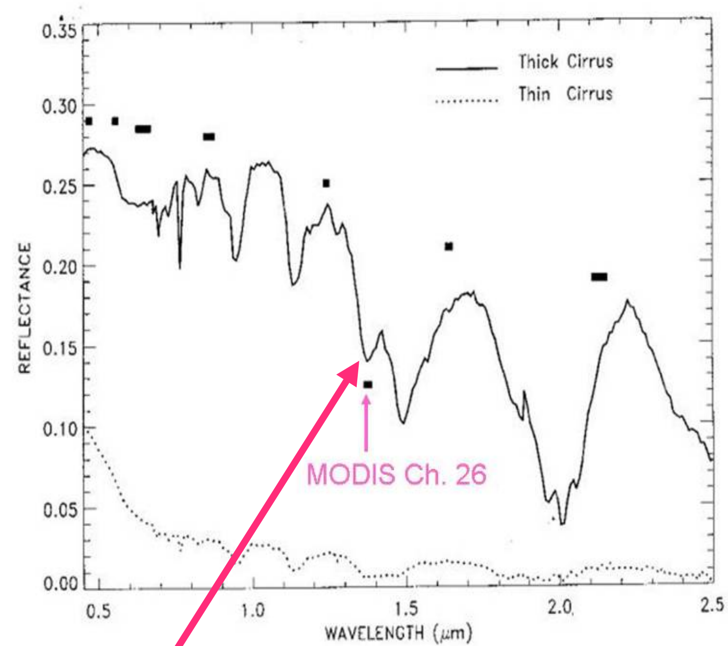


The water vapor absorption effects (in the sun-cirrus-sensor path) need to be corrected before the 1.38-micron image can be used for removing cirrus effects in images of other channels.

# Estimates of the MODIS 1.375-μm Channel Water Vapor Transmittance by Dividing a Large MODIS Scene into 4 x 4 Smaller Blocks

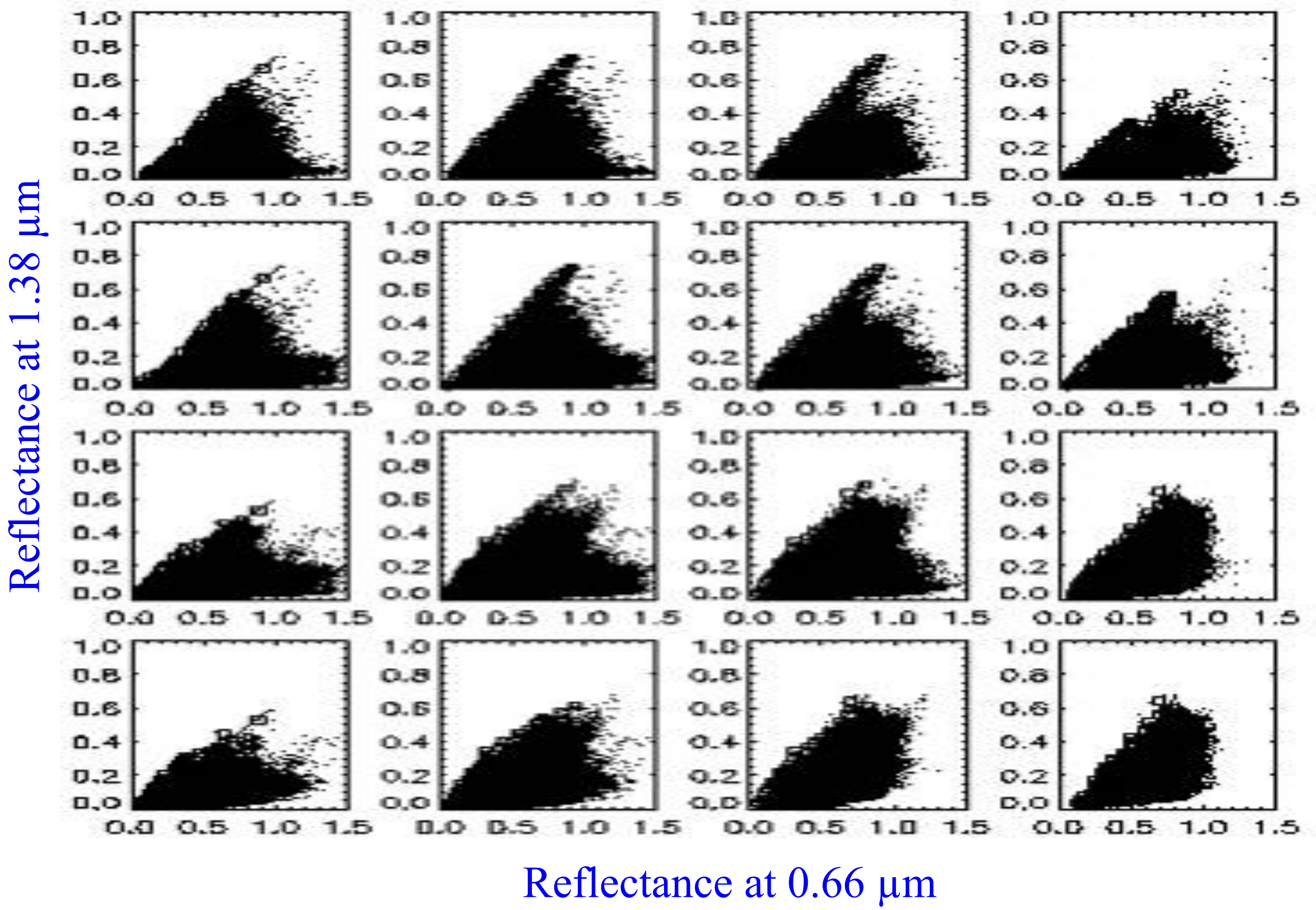


The slope of a line in the upper left edge portion of a scatter plot is a good estimate of the water vapor transmittance factor. We cannot solve for T(1.38) on a pixel-by-pixel basis, and we have to use spatial information. The scatter-plot approach was developed in early 1990s after private discussions with Dr. Yoram Kaufman.

# Equations for the Derivation of Cirrus Reflectances Using a Scatter-Plot approach & Cirrus Corrections

The apparent reflectance at the satellite level is defined as:

$$\rho^*_\lambda = \pi L_\lambda / (\mu_0 E_{0\lambda})$$

$$\rho^*_\lambda = \rho_{c\lambda} + T_{c\lambda} \rho_\lambda / (1 - S_{c\lambda} \rho_\lambda) \qquad (1)$$

$\rho_{c\lambda}$ : path radiance due to cirrus;

$S_{c\lambda}$: cloud scattering of upward radiation back to surface;

$\rho_\lambda$ : Surface reflectance;

If $S_{c\lambda} << 1$, Eq. (1) becomes: $\rho^*_\lambda = \rho_{c\lambda} + T_{c\lambda} \rho_\lambda$ (2)

We found an empirical relation: $\rho_{c\lambda} = \rho_{c1.375} / K_a$ (3)

where $K_a$ = Sun-cirrus-sensor vapor transmittance at 1.375 μm. It is derived empirically from a scatter plot.

Substituting Eq. (3) into (2), we get

$$T_{c\lambda} \rho_\lambda = \rho^*_\lambda - \rho_{c1.375} / K_a$$

(4)

To a good approximation: $T_{c\lambda} = 1 - \rho_{c\lambda}$

& $\rho_\lambda = (\rho^*_\lambda - \rho_{c1.375} / K_a) / (1 - \rho_{c1.375} / K_a)$

(5)

# An Example of MODIS Cirrus Detection and Correction

MODIS Original RGB Image

1.38-μm MODIS Image

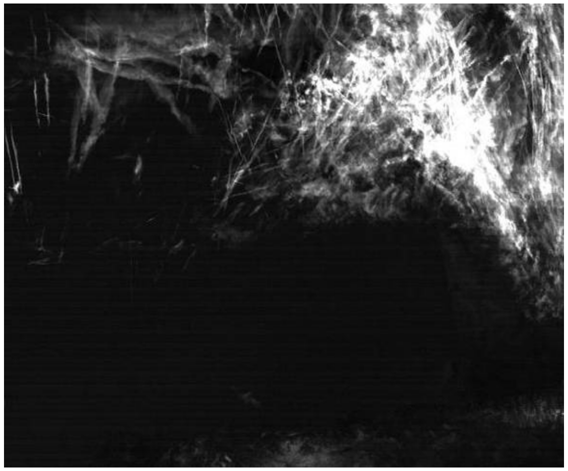

Cirrus-Corrected RGB Image

The horizontal striping effects in the 1.38-micron image are introduced in the cirrus-corrected RGB image.

# An Example of VIIRS Cirrus Detection & Cirrus Removal Over Red Sea

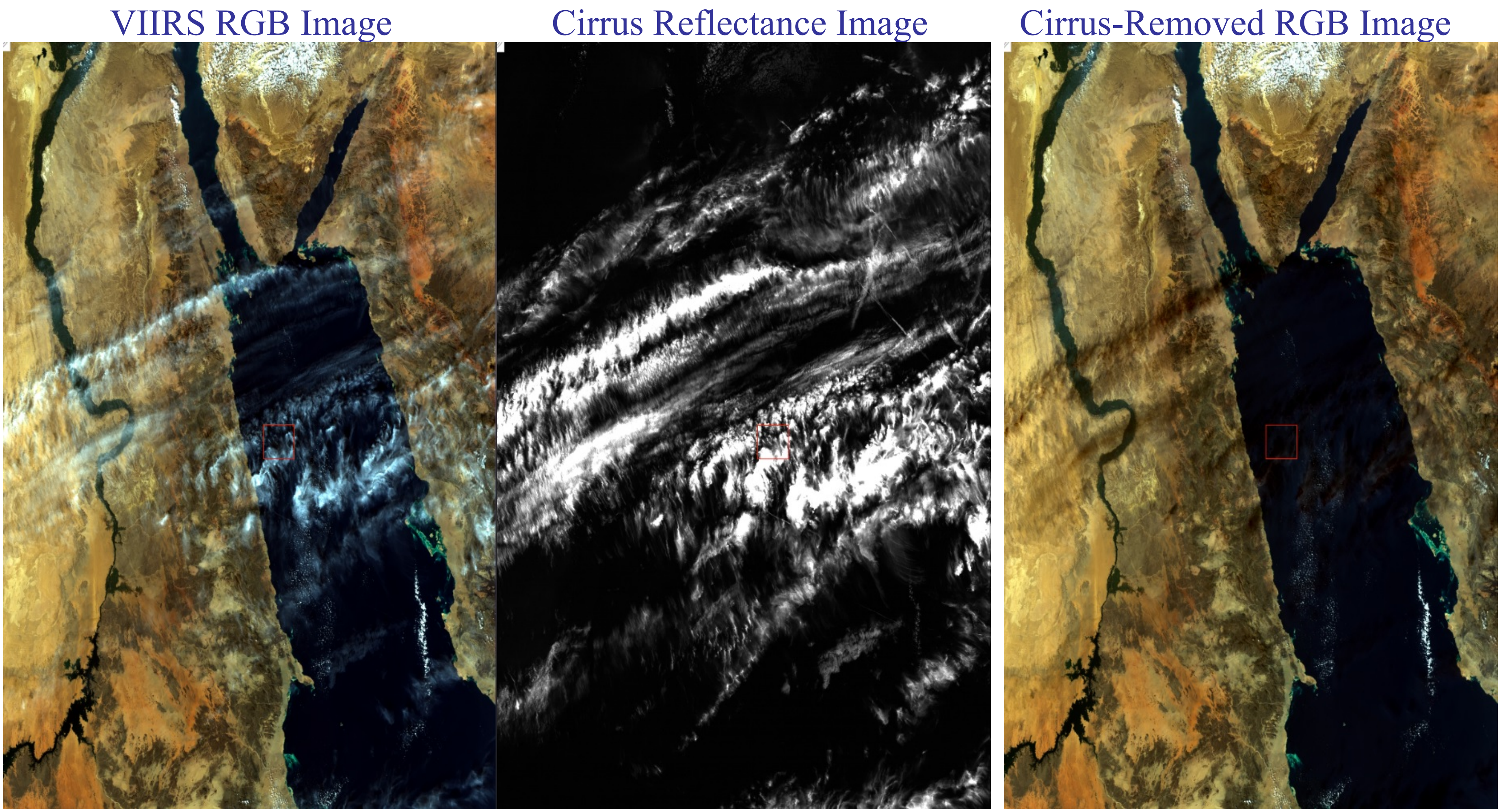


No horizontal striping effects are introduced in the cirrus-corrected RGB image.

# Cloud Detection At High Latitude Regions

VIIRS RGB Image

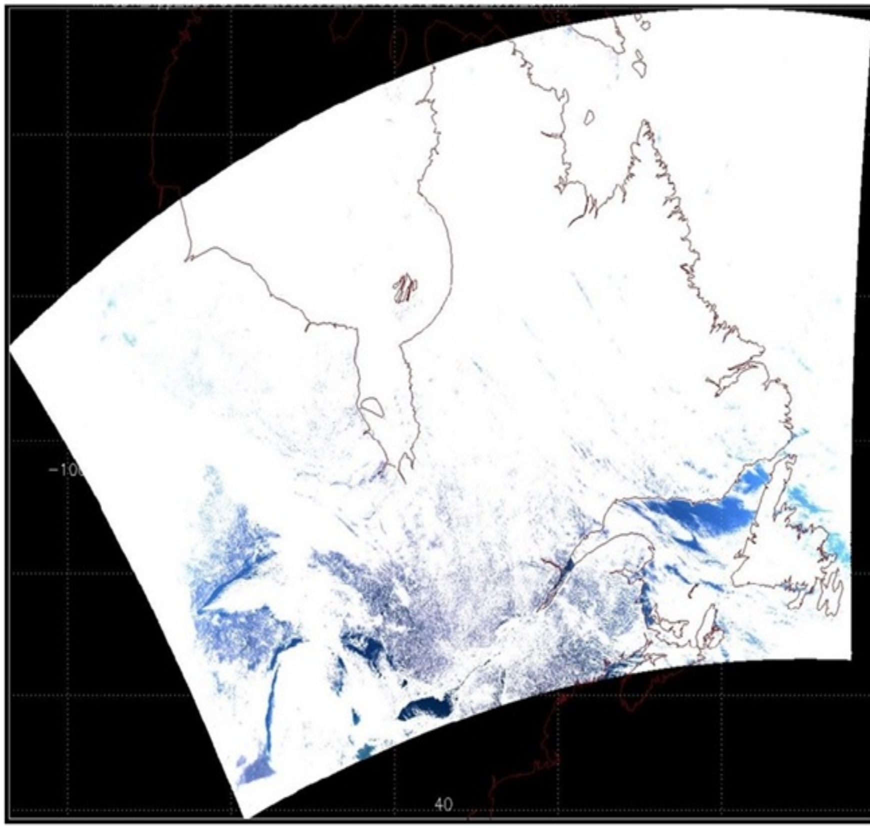


VIIRS M9 Image

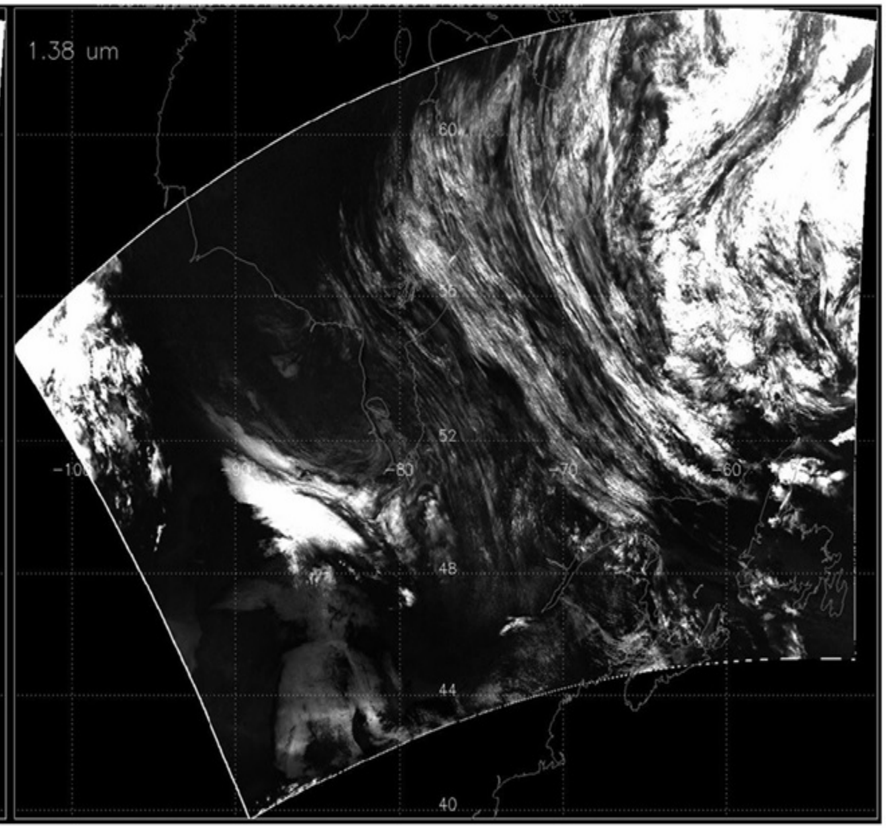

# Volcanic Ash Detection

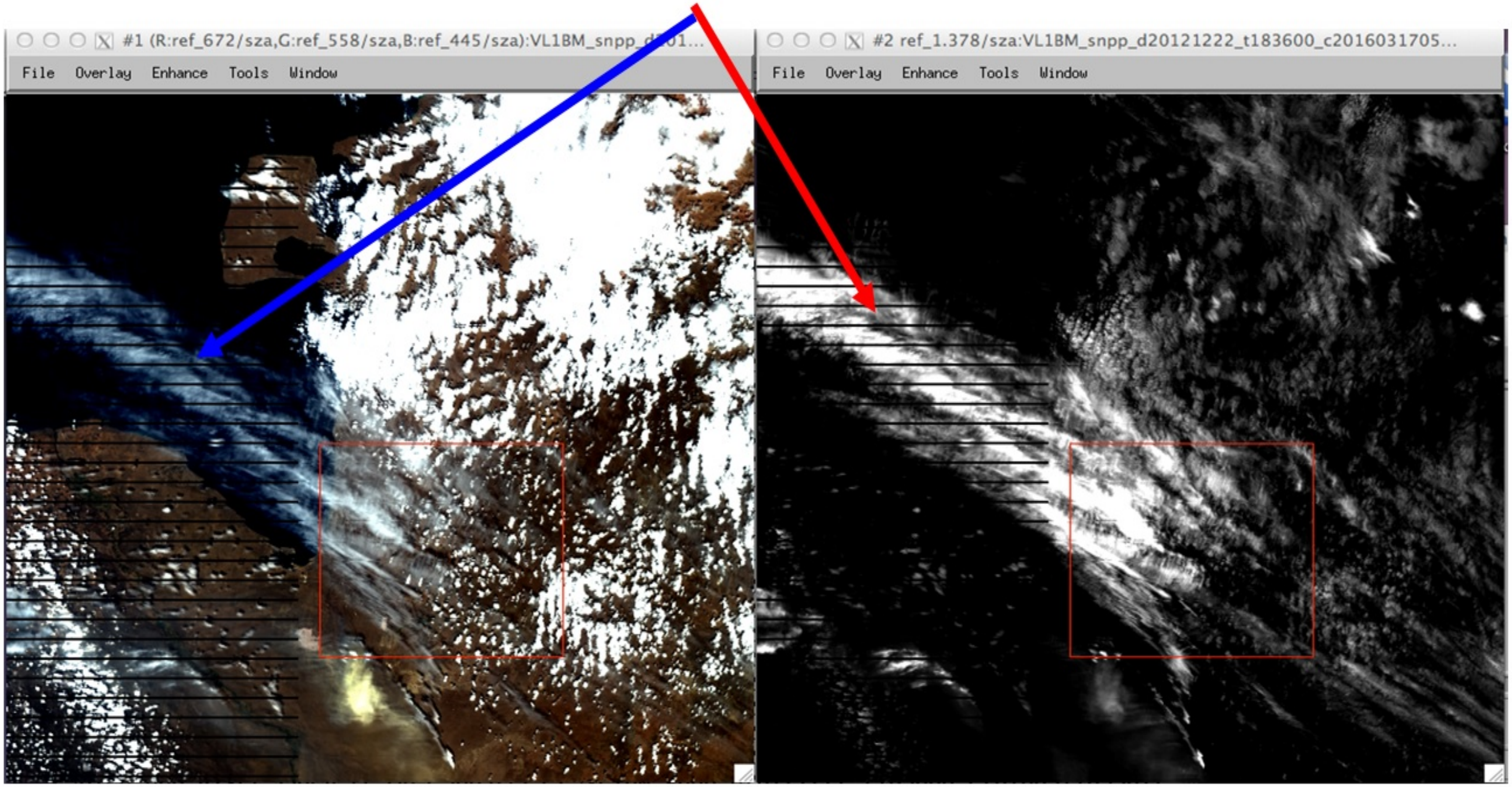


Gao, B.-C., and Y. J. Kaufman, Selection of the 1.375-μm MODIS channel for remote sensing of cirrus clouds and stratospheric aerosols from space, *J. Atm. Sci., 52*, 4231-4237, 1995.

# Cloud Detection Over Water, Sunglint, and Desert Areas

VIIRS RGB Image

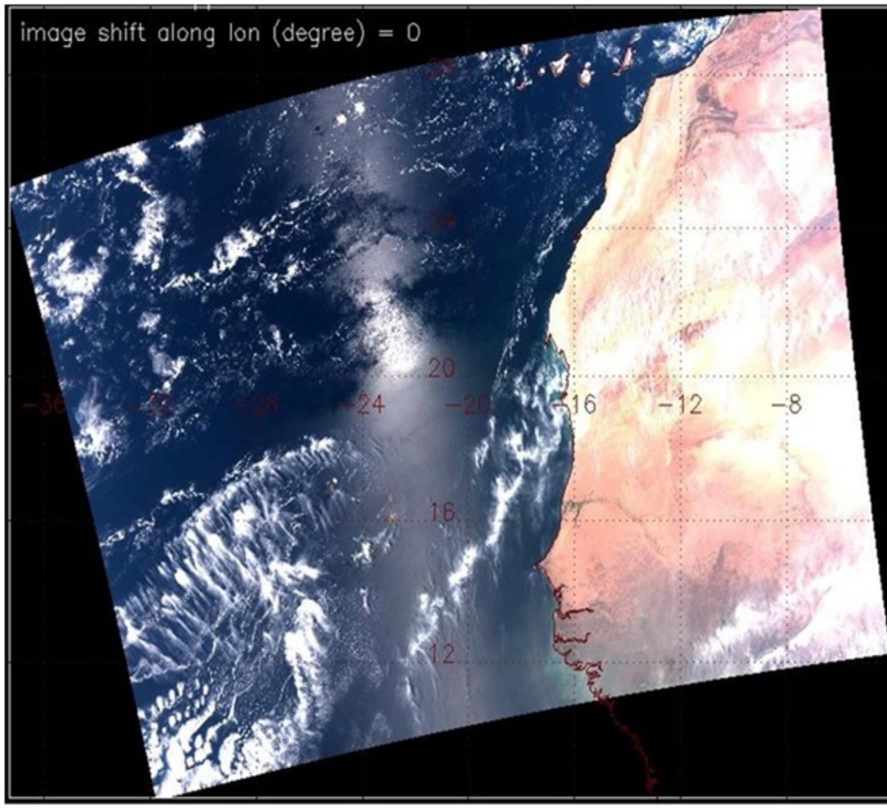


VIIRS M9 Image

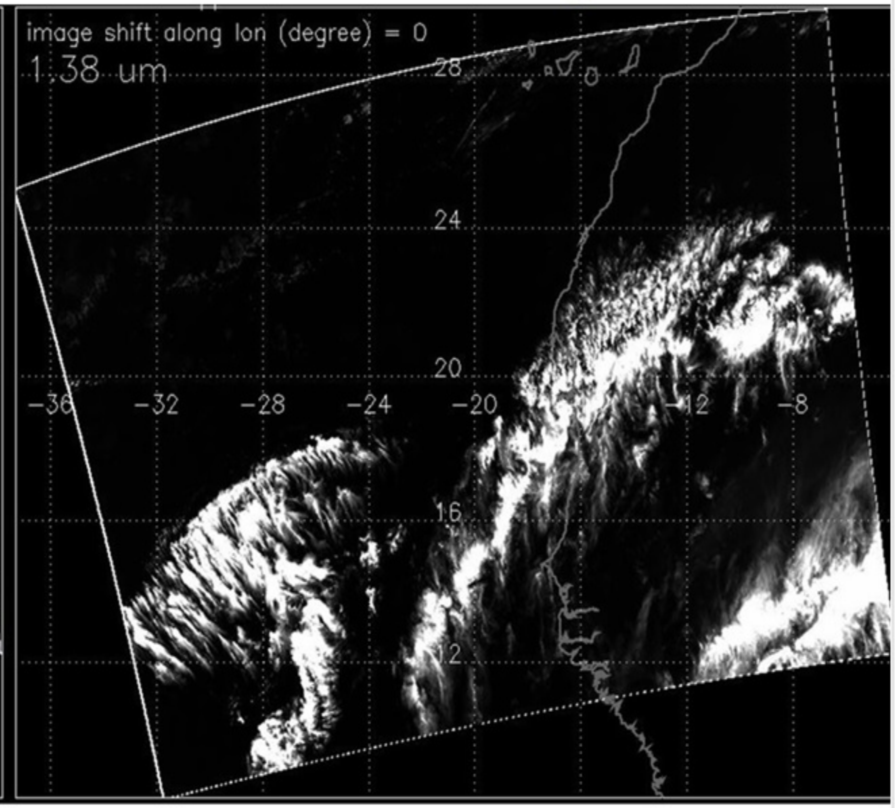

# Cloud Detection Over Tibet During A Dry Season

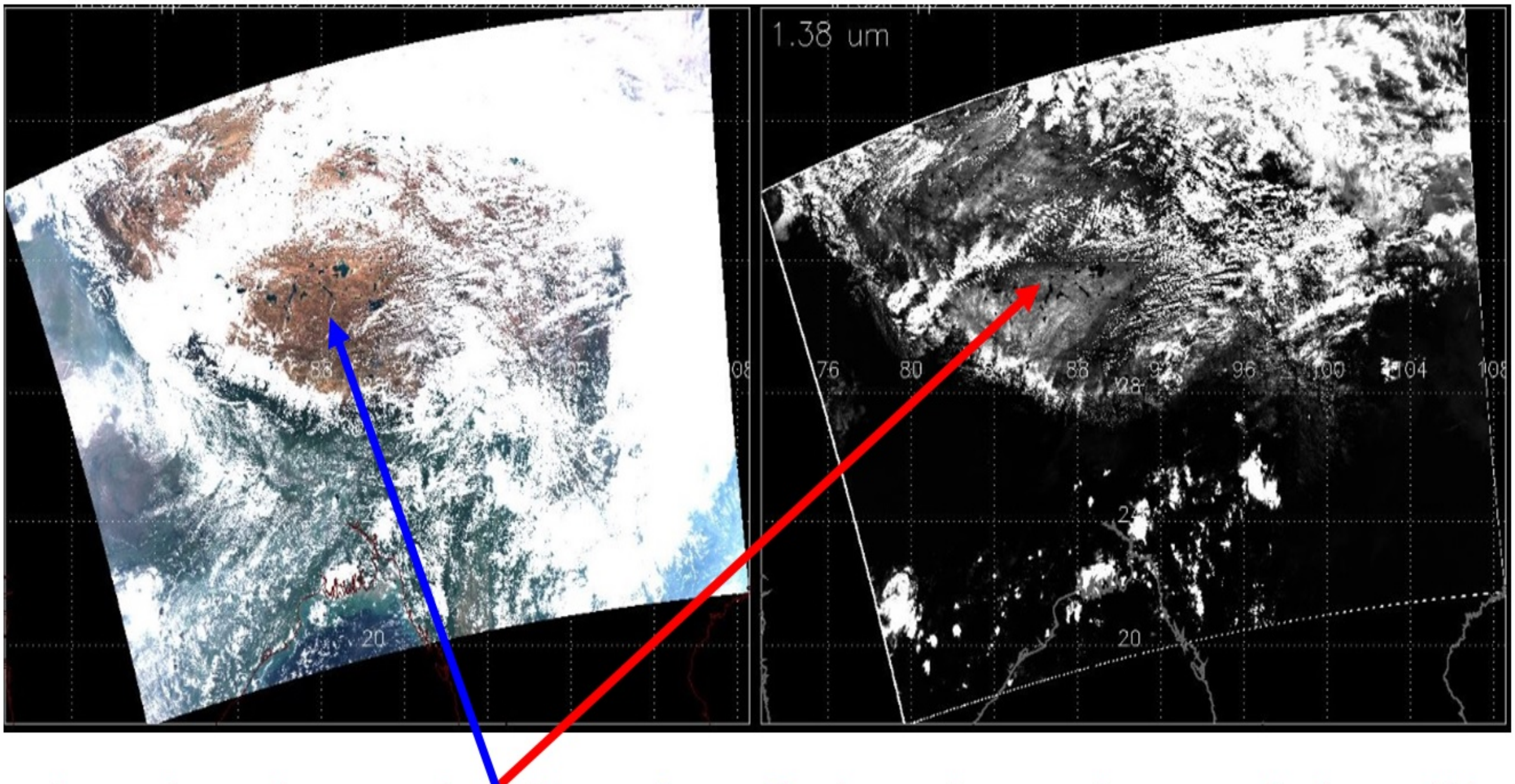


The M9 image is contaminated by surface reflection under very dry atmospheric condition.

# An Example of Landsat 8 OLI Cirrus Detection and Correction

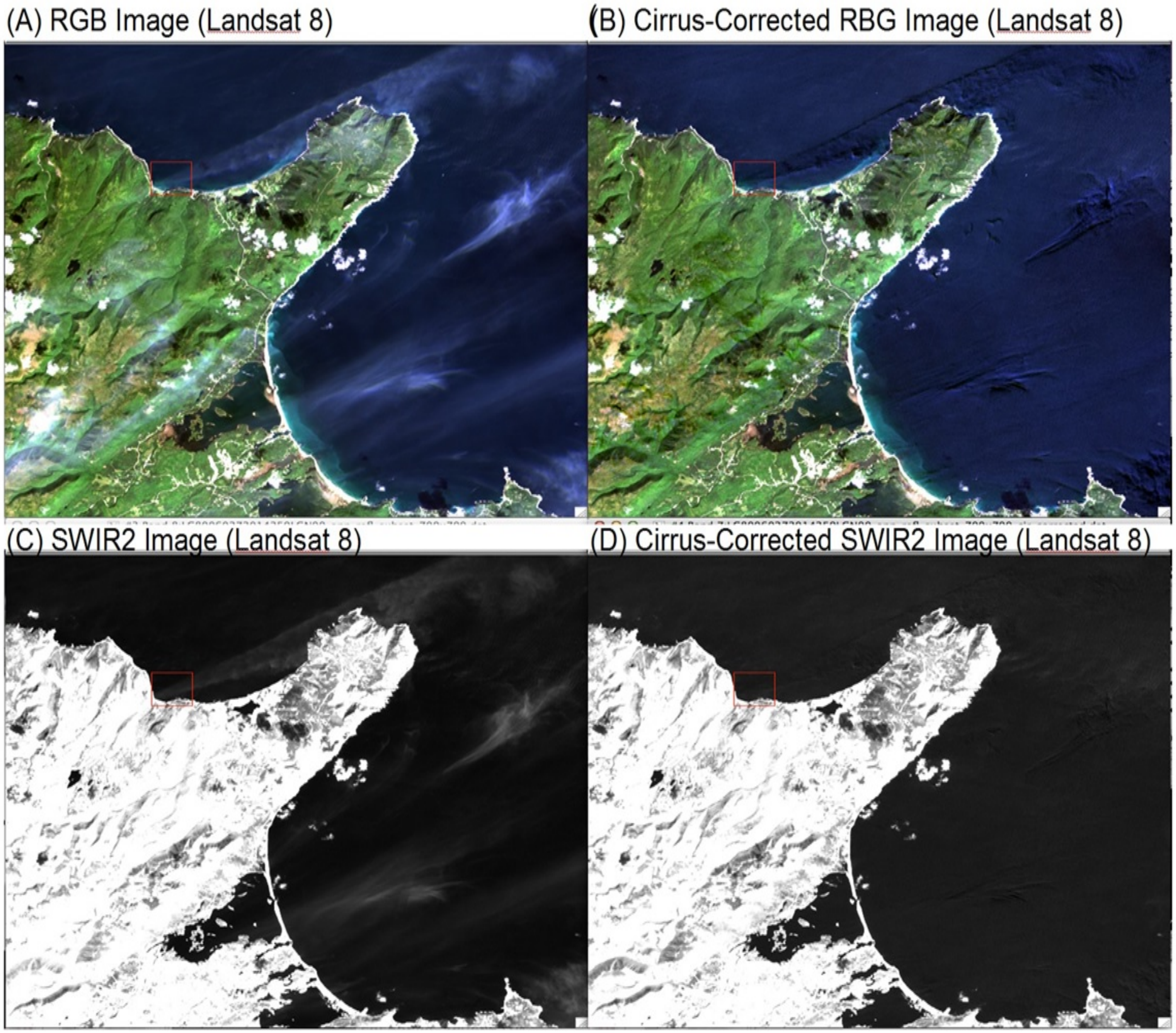

# Taking Consideration of Filter Function Differences Between VIIRS M9 and MODIS Ch. 26

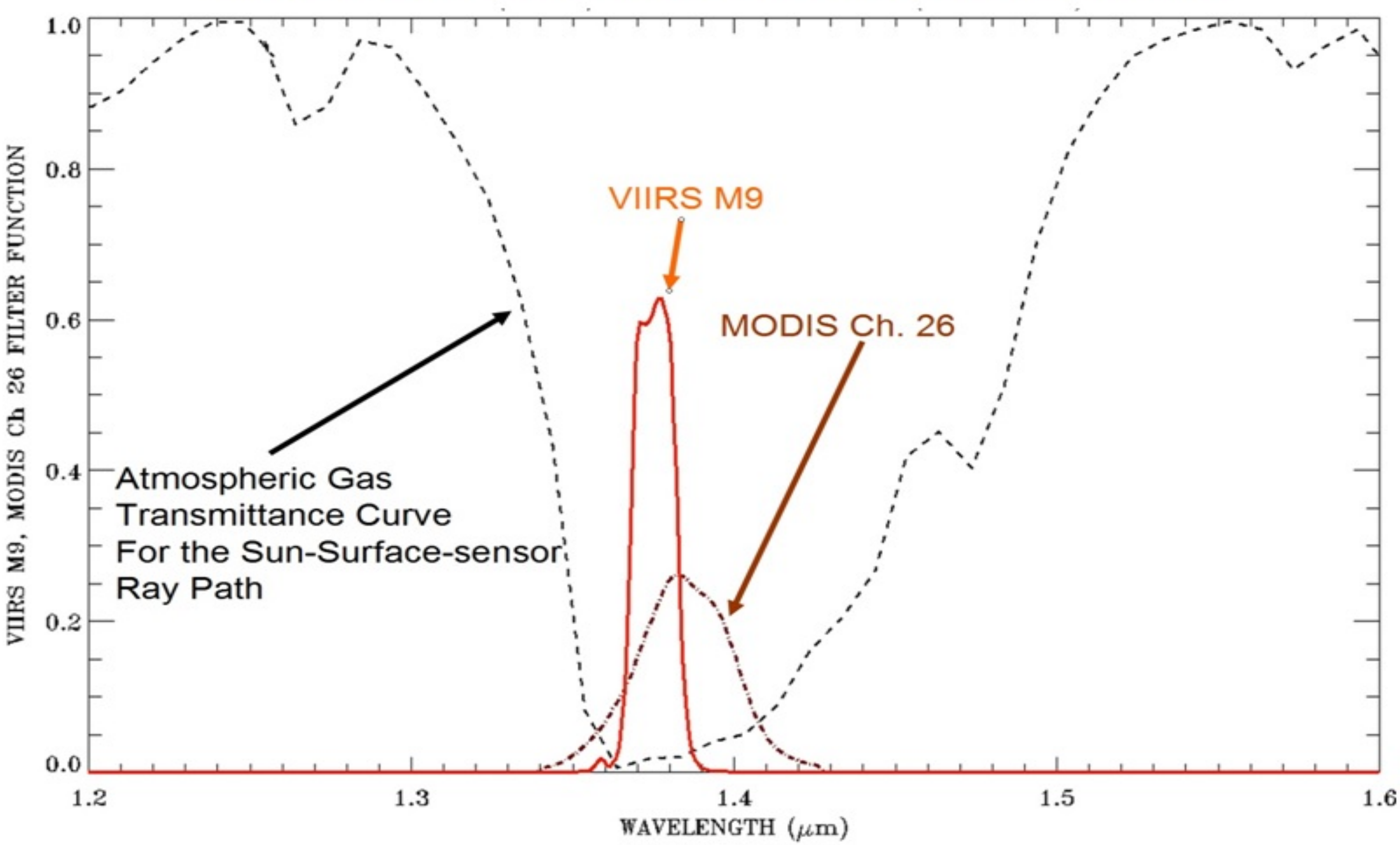

# Improvement to the VIIRS Cirrus Reflectance Algorithm

## Improving The Selection of Default Values of Upper Level Water Vapor Transmittances Using Simulated VIIRS M9 Transmittances As a Function of Solar and View Angles

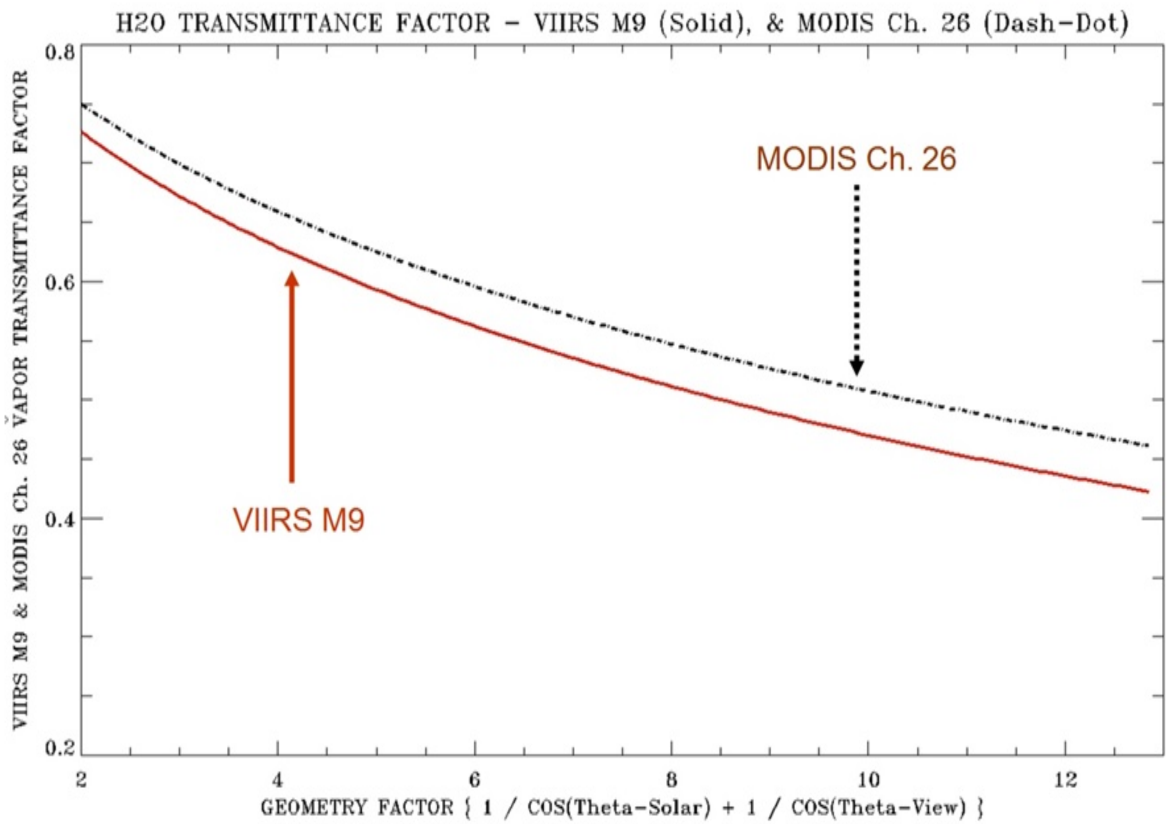

# Improvement to the VIIRS Cirrus Reflectance Algorithm

## Developing A New Algorithm for Estimating the Upper Level Water Vapor Transmittance Factor from the Scatter Plot of VIIRS M9 Sub-Image Versus M5 Sub-Images

(A) VIIRS M9 Sub-Image

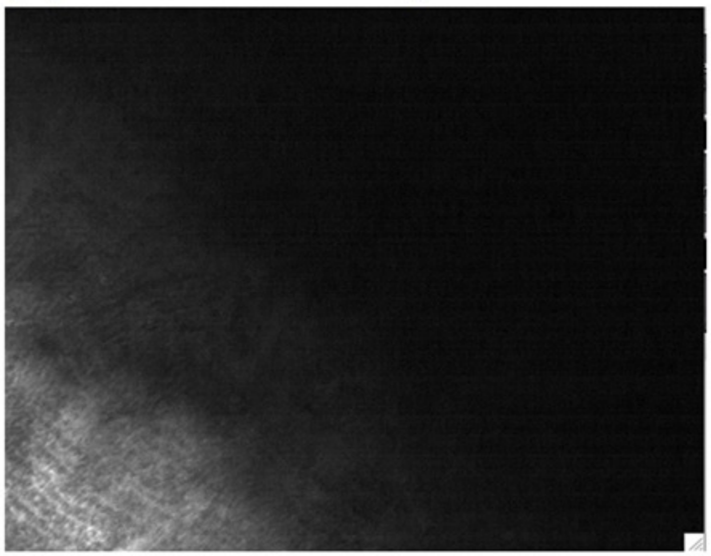

(B) Scatter Plot of M9 VS M5 Channels

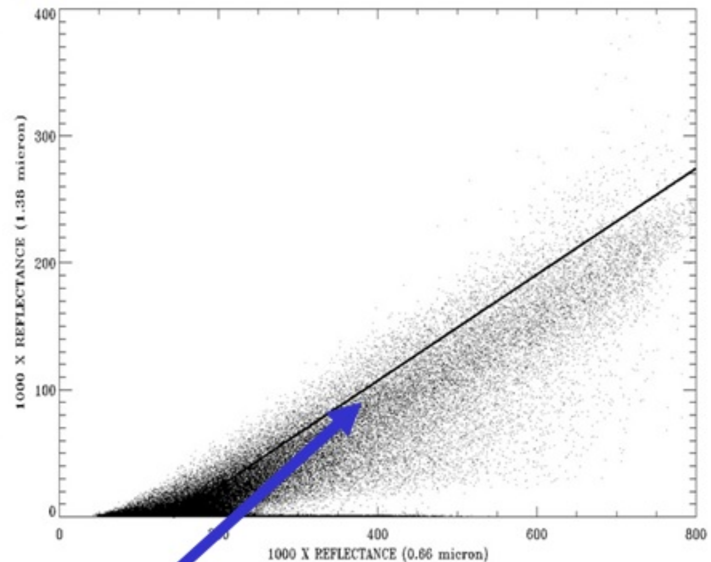


The slope of this straight line is the best estimate of the upper Level water vapor transmittance factor.

# SUMMARY

Because M9 is the only VIIRS channel located in atmospheric gas absorption regions and because the rest of VIIRS channels are located in atmospheric "*window*" regions, M9 offers the unique capability in remote sensing of clouds from space. We have found that M9 channel is very useful in daytime detection of thin clouds over snow- and ice-covered polar region. M9 can also detect volcanic ash during the daytime. M9 is not affected by sunglint over water surfaces. However, under very dry atmospheric conditions over elevated surfaces, such as the Tibet Plateau in winter months, M9 can receive solar radiation reflected from the bottom surface. We made major improvements to the VIIRS cirrus reflectance algorithm. We took into consideration of the M9 channel filter function, which is different from the filter function of MODIS channel 26, in the updated VIIRS cirrus reflectance algorithm. We also developed and implemented a more stable routine to estimate the upper level water vapor transmittance along the Sun-cirrus-VIIRS ray path from the scatter plot of M9 (1.378 micron) versus M5 (0.672 micron) images. We partially relied on the high spatial resolution Landsat8 OLI data to guide the development and validation of the new routine. We described briefly the history of MODIS cirrus detecting channel, the improvement in the VIIRS version of cirrus reflectance algorithm, and presented sample results from Landsat8 OLI data and VIIRS data. At present, the output does not contain QA parameters and error and uncertainty estimates. The QA routines need to be developed and implemented in the future.